Supporting Information

Blanchet et al. 10.1073/pnas.1715578115

SI Materials and Methods

Strains and Plasmids. All of the strains used in this study were derived from 74-D694 (mata ade1-14 [UGA] ura3-52 trp1-289 [UAG] his3Δ200 leu2-3,112 [*PSI*$^+$]). Readthrough GST proteins were expressed and purified in the [*PSI*$^+$] ΔUPF1 strain (the parental strain) transformed with pYX24-GST, as previously described (16). Other groups have confirmed that the genetic background of this strain does not influence the ratio of amino acids incorporated at stop codons (30). For this reason, the parental strain is refered to as WT in the report. The three stop codons have been inserted either in the GST or the dual β-galactosidase/luciferase reporters in the context of the *IXR1* gene, as previously described (16). The genes encoding the various enzymes modifying the tRNAs were deleted in this strain by insertion of the *HIS3* cassette by homologous recombination. The phenylalanine tRNA was overexpressed in ΔTRM7 to ensure viability. For growth rate analysis, strains were grown in rich medium (YPD) at 30 °C until stationary phase. The ΔPUS7ΔMOD5 double mutant was constructed by replacing the *MOD5* gene with a NAT deletion cassette in the ΔPUS7 strain. The resulting mutant is selected on YPG agar supplemented with 100 μg/mL nourseothricin. The D256A mutation was introduced into the *PUS7* gene by site-directed mutagenesis. PUS7wt and PUS7-D256A were produced with the pFL36 vector (pARS/CEN, *LEU2*).

Mass Spectrometry.

Sample preparation. GST-purified proteins were separated by SDS/PAGE and stained with Coomassie brilliant blue. Bands corresponding to GST proteins were excised and subjected to enzymatic digestion. Briefly, protein bands were excised and thoroughly washed with 100 mM ammonium bicarbonate/acetonitrile [1:1 (vol/vol)]. The excised bands were treated with 100 μL 10 mM DTT at 56 °C for 30 min. The DTT was removed and 100 μL of 55 mM iodoacetamide was added for cysteine carbamidomethylation. The reaction was allowed to proceed at room temperature for 30 min. The supernatant was removed, the washing procedure was repeated and the gel slices were dried. We added 20 μL of 10 ng/μL LysN (Thermo Scientific Pierce) in 25 mM NH_4HCO_3, and the mixture was incubated overnight at 37 °C. Peptides were extracted in 50% acetonitrile and 0.1% (vol/vol) formic acid, dried under vacuum, and then resuspended in 5% formic acid to prevent the loss of hydrophobic peptides before LC-MS/MS analyses.

LC-MS/MS analyses. Proteolytic peptides were further identified and quantified with a Triple-TOF 4600 mass spectrometer (ABSciex) coupled to the nanoRSLC system (Thermo Fisher Scientific) equipped with a trap column (Acclaim PepMap100C18, 75 μm i.d. × 2 cm, 3 μm) and an analytical column (Acclaim PepMapRSLCC18, 75 μm i.d.× 25 cm, 2 μm, 100 Å). Peptides were eluted with an acetonitrile gradient of 5–35% (vol/vol) over 40 min, at a flow rate of 300 nL/min. MS/MS spectra were acquired by a data-dependent acquisition method involving the selection of the 20 precursors giving the most intense signals, CID fragmentation with the Q1 quadrupole set at low resolution to improve sensitivity. Raw data were processed with MS Data Converter software and analyzed with PeakView software (ABSciex) (Fig. S2).

Protein identification. Proteins were identified with the MASCOT algorithm and an in-house database was constructed by merging Swissprot with user-generated GST sequences, each harboring one of the 20 amino acids at the readthrough site. The other search parameters were as follows: digest reagent LysN (cleavage at the N terminus of lysine), cysteine carbamidomethylation was considered a complete modification, and oxidation (methionine and tryptophan) was considered variable. Peptide and fragment tolerances were set at 10 ppm and 0.05 Da, respectively. Only ions with a score higher than the identity threshold corresponding to a false-positive discovery rate of 1% (Mascot decoy option) were considered.

Relative quantification of readthrough peptides. MS extracted-ion chromatograms (XIC) were generated for the peptides harboring readthrough amino acids. The intensity of each chromatographic peak was corrected by a factor taking the ionization and digestion efficiencies of each readthrough peptide into account (16). The means of three technical replicates are reported. We determined whether a decrease in the relative intensities of readthrough peptides affected by the elimination of tRNA modifications was compensated by the incorporation of other amino acids at the stop codon, by dividing the absolute intensities of readthrough peptides by the mean intensity for the three most intense internal peptides and comparing the results in different conditions with those obtained in control conditions.

tRNA Quantification. To selectively quantify mature tRNA in *Saccharomyces cerevisiae* strains, we proceeded following the RNA Biology communication from the Kirino group (23). To amplify specific tRNA by Taqman qPCR using Premix Ex Taq (Clontech Lab), we deacylated total RNA to anneal and ligate an adapter to tRNA, followed by the specific synthesis of cDNA from the ligated tRNA and 5S rRNA used as internal control. The 5S rRNA expression was quantified by qPCR using SsoFast EvaGreen Supermix (Bio-Rad) on 10× serial dilution of cDNA. The tRNA relative quantity was expressed referred to the 5S rRNA and then normalized to the quantity of glutamine tRNA.

We used the primers listed in Table S2.

RNA-Seq and Ribosome Profiling. Cells were grown to an OD_{600} of 0.6 in 1 L of liquid glucose-YNB supplemented with CSM and 2× adenine and flash-frozen. Total RNA and polysomes were extracted as previously described (5, 6). The polysome profile was checked by the separation of an aliquot on a linear sucrose gradient (7–50%). Ribosome-protected mRNA fragments (RPFs) were generated by the treatment of 1 OD_{260nm} unit of extract with 15 U of RNase I for 1 h at 25 °C, and digestion efficiency was checked on a sucrose gradient. RNA was purified by phenol extraction and 28-nt RPFs were recovered by electrophoresis in a 17% acrylamide (19/1) gel. These RPFs were depleted of ribosomal RNA by treatment with the Ribo-Zero Gold rRNA removal kit for yeast from Illumina. RPF libraries were generated with an NEBNext Small RNA Sample Prep Kit, according to the manufacturer's protocol, and were checked with the bioanalyser small RNA kit. Sequencing was performed by a NextSEq. 500 (Illumina) 75-nt single-read protocol.

Raw Data to Alignment Files (BAM). Raw reads from RIBO-seq were first subjected to quality control with FastQC software, and were then trimmed with CutAdapt to remove 3′ adapters (-a) and apply a quality threshold (-q 30). Trimmed reads were aligned with the sequences in the yeast rRNA database (SGD), with the Bowtie aligner. Only unmapped reads were kept (- - unmapped). Finally, filtered reads were aligned with the Saccer3 genome, with Bowtie, allowing up to two mismatches (-n 2) and retaining uniquely mapped reads (-m 1). The generated alignment files (SAM) were converted to BAM format and manipulated with Samtools.

Per Codon Analysis. We selected 28- to 29-nt-long reads. The first nucleotide in the ribosome A site was defined as the +15 position relative to the 5′ end of the read. Based on SACCER3 [SGD(3)] genome annotation, only reads mapping to coding sequences (CDS) for which the nucleotide in the A site was in-frame with the CDS were collected. We then calculated codon coverage separately for each gene by: (*i*) counting the number of A sites on each codon of the CDS (codons with fewer than two reads were discarded), (*ii*) normalizing by dividing by gene size in nucleotides, (*iii*) normalizing by dividing by the database size, and (*iv*) averaging the normalized counts for each identical codon of the CDS. The *P* value was calculated using student test with $\alpha = 0.05$.

Stop Codon Readthrough Detection. We extracted from the reference genome all of the 3′ extensions (between the stop of the CDS and the next in-frame stop codon) longer than 9 nt. We counted the number of 28-mers reads that are in-frame with the official CDS in this extension. This value is normalized with the length of the 3′ extension and the size of the dataset to obtain the density of 28-mers reads within the extension. The *P* value was calculated using student test with $\alpha = 0.05$.

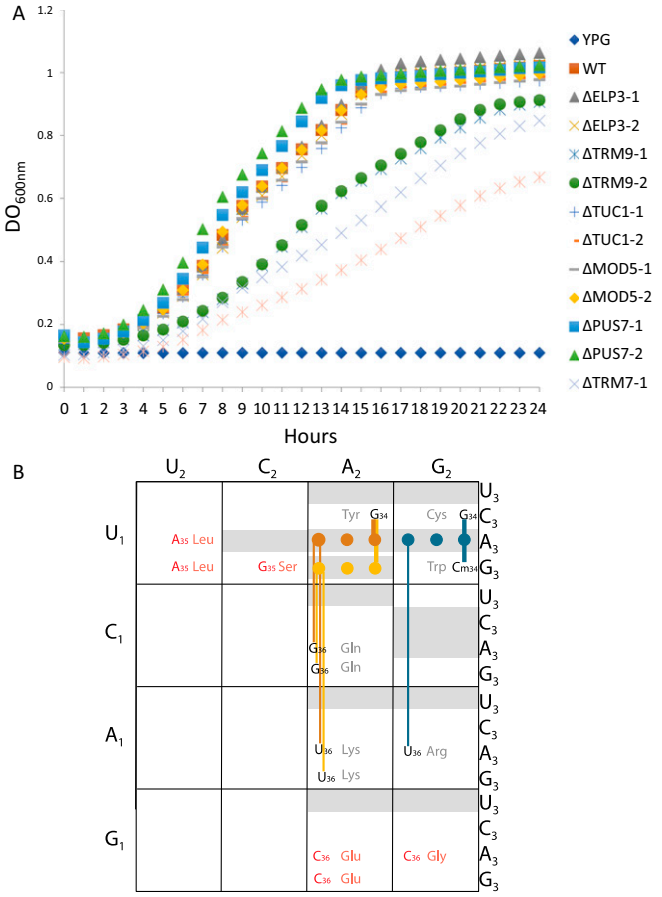

Fig. S1. (*A*) The growth curves of all of the strains used in this study. Two mutants were tested for each gene, to eliminate reproducibility issues. (*B*) A genetic code table. Each stop codon is represented by their respective color: ochre, opal, and amber. Only nucleotides within the tRNA that make an unconventional base pairing are indicated. Mismatches that have been never found are indicated in red; gray boxes indicate that the corresponding tRNA does not exist in the genome of *S. cerevisiae*.

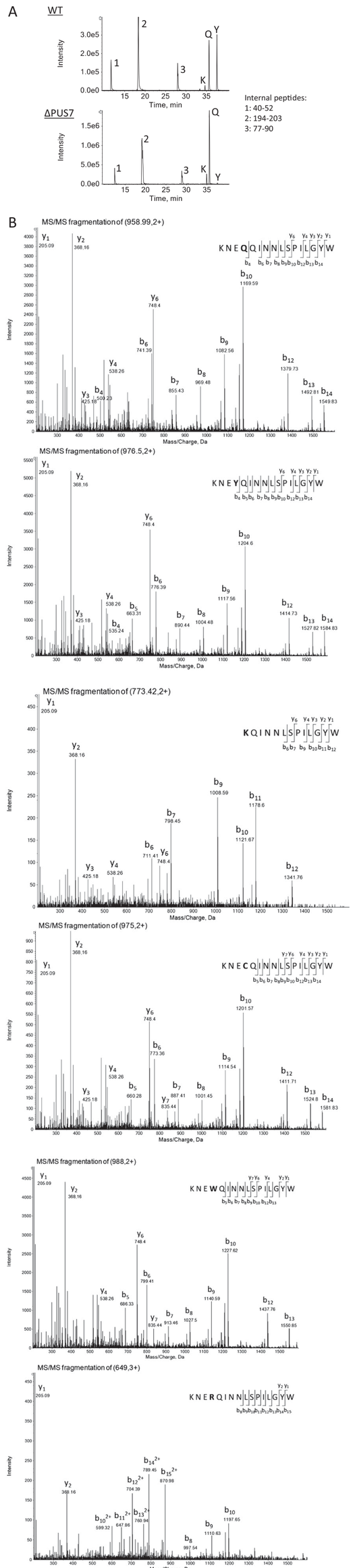

Fig. S2. (*A*) Evaluation of compensation effects for readthrough amino acids affected by the abolition of tRNA modifications. MS extracted-ion chromatograms for readthrough peptides and the three most intense internal peptides from GST analysis are shown for the UAA stop codon in the WT and ΔPUS7 strains. In the example shown, a strong decrease in the intensity of the readthrough peptide containing Y is entirely compensated by better incorporation of Q and K. Example calculation of the normalized intensity of the readthrough peptide containing Q. WT: $3 \times I(Q)/[I(1) + I(2) + I(3)] = 0.42$; ΔPUS7: $3 \times I(Q)/[I(1) + I(2) + I(3)] = 1.08$ (Abbreviation: I, Intensity on extracted-ion chromatogram.). (*B*) MS/MS spectra for readthrough peptides. Panels show representative Triple-TOF MS/MS spectra for readthrough peptides, for the UAA/UAG and UGA stop codons, in the WT strain. The identified fragments are annotated on the sequence and the Mascot ion scores (not shown) of readthrough peptides were significantly higher than the identity thresholds calculated for a false-discovery rate of 1%.

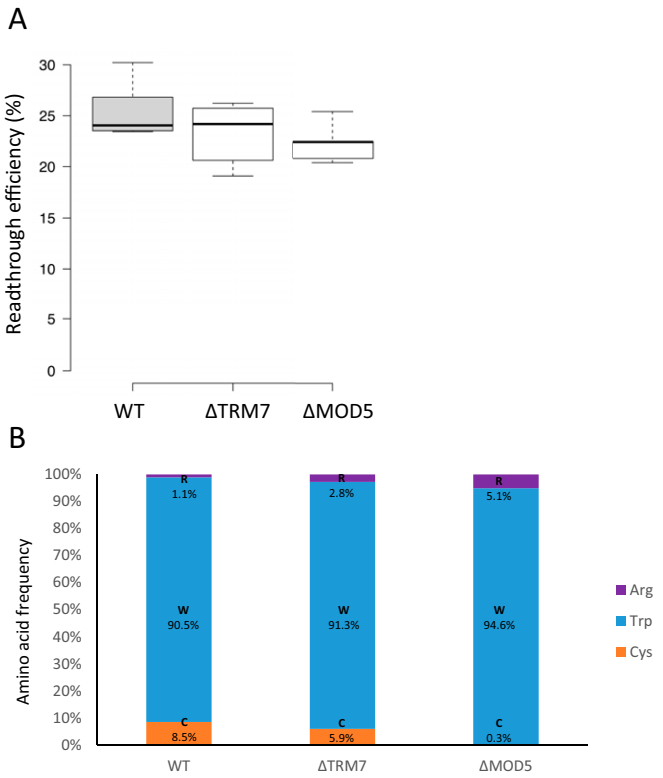

Fig. S3. (*A*) Quantification of readthrough efficiency at the UGA codon in the ΔTRM7 and ΔMOD5 strains. At least five independent experiments were performed for each value. The lines in the center correspond to the medians; box limits indicate the 25th and 75th percentiles as determined by R software; whiskers extend to 1.5 times the interquartile range from the 25th and 75th percentiles. (*B*) Quantification of the relative proportions of the amino acids identified at the UGA codon. Intensities (corrected by a factor taking the ionization and digestion efficiencies of each readthrough peptide into account) of readthrough peptides normalized according to the amount of GST. Relative frequencies of the amino acids incorporated at stop codons were determined by calculating the mean values for three experiments. Quantification was performed as described in *Materials and Methods*.

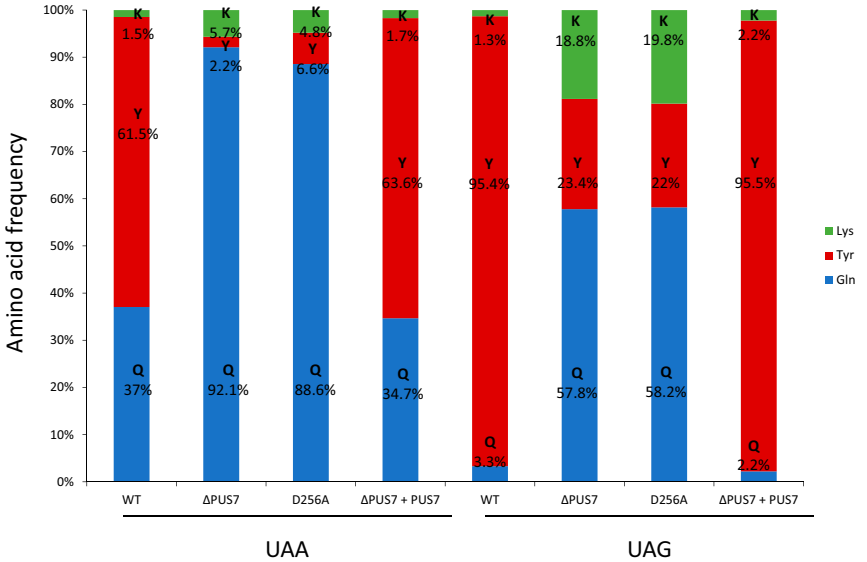

Fig. S4. Quantification of the relative proportions of the amino acids identified at the two stop codons. Intensities (corrected by a factor taking the ionization and digestion efficiencies of each readthrough peptide into account) of readthrough peptides normalized according to the amount of GST. The relative frequencies of the amino acids incorporated at stop codons were determined by calculating the mean value for three experiments. Quantification was performed as described in *Materials and Methods*.

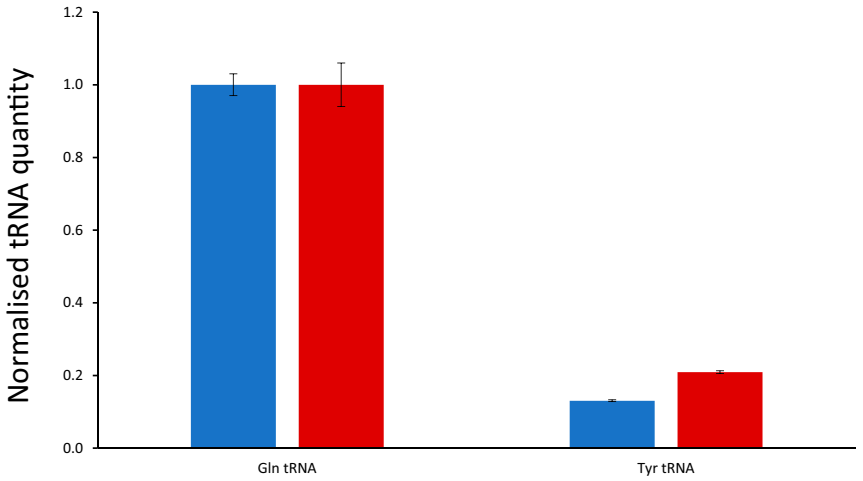

Fig. S5. Quantification of Tyr and Gln tRNAs in WT and Δpus7 strains. The 5S rRNA is used to normalize the amount of each tRNA species. Gln tRNA quantity is used as an internal control because it is not modified by Pus7p. $n = 10$ for all of the samples.

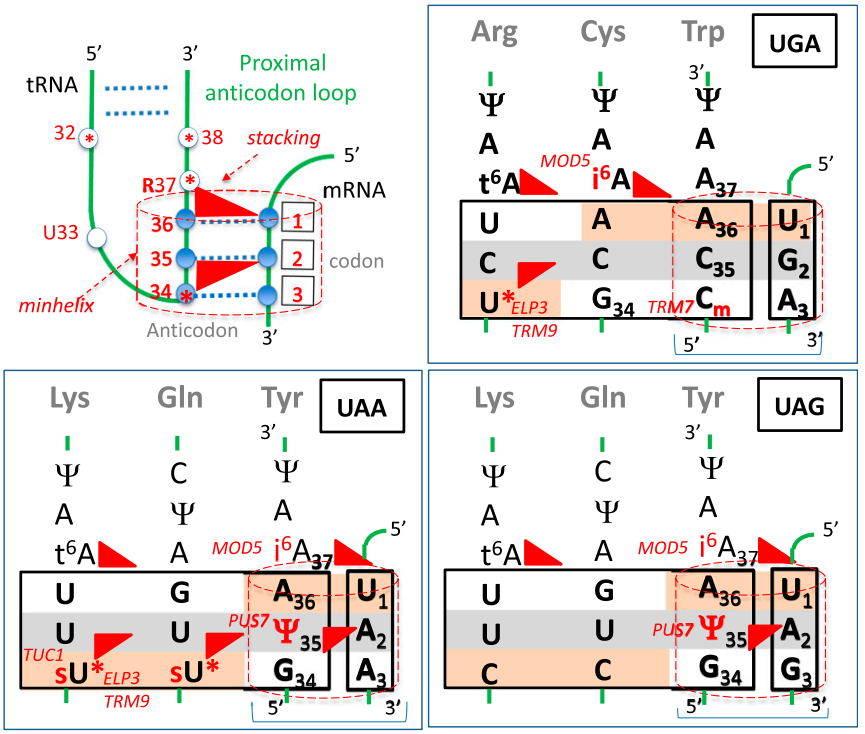

Fig. S6. Codon–anticodon interacting systems between stop codons and suppressor tRNAs. On the *Upper*, *Left*, the proximal anticodon loop of tRNA (from nucleotide 20 to nucleotide 40) is schematized. The three bases (1-2-3) of the codon in mRNA interact with the three bases of anticodon (34-35-36) in tRNA forming a minihelix with the Watson–Crick-type geometry. Red triangles symbolize the additional stabilization by stacking of adjacent base pair due to the presence of chemical adducts to base or ribose. Asterisks (*) represent mcm^5 modification. Acronyms of modified nucleotides and corresponding modification enzymes in yeast are indicated in red. Within each of the three stop codon boxes, bases in the anticodon that mismatch with one of the three bases of stop codon are highlighted under white background, while those involved in standard Watson–Crick helices are under orange backgrounds.

Table S1. Identification of readthrough peptides

Stop codon	Identified readthrough peptides	Peptide mass (Da)	Retention time (min)
UAA UAG	KNE**Q**QINNLSPILGYW	1,915.97	35.5
	KNE**Y**QINNLSPILGYW	1,950.98	37.5
	KQINNLSPILGYW	1,544.83	34.5
UGA	KNE**C**QINNLSPILGYW	1,947.95	36
	KNE**W**QINNLSPILGYW	1,974.00	40
	KNE**R**QINNLSPILGYW	1,944.02	31.5

This table summarizes the readthrough peptides unambiguously identified by LC-MS/MS analyses for the three stop codons. Amino acids incorporated at readthrough sites are shown in bold. All of the cysteine residues found were carbamidomethylated. Masses were determined to within 5 ppm for all mass measurements.

Table S2. Primers used for the FL–qRT-PCR

Name	Sequence (5′-3′)
SL-Adaptor-Gln	/5Phos/TCGTAGGGTCCGAGGTATTCACGATGrGrA
SL-Adaptor-Tyr	/5Phos/TCGTAGGGTCCGAGGTATTCACGATGrGrU
Cyto-tRNAGln-RT/R	CCGAAAGTGATAACCACTACACTATAGGACC
Cyto-tRNAGln-F	CGGTTCGAATCCGGGTAGGAC
Cyto-tRNATyr-RT/R	TCTTGCGCCTTAAACCAACTTGGCTACCGAGAG
Cyto-tRNATyr-F	CGTTCGACTCGCCCCCGGGA
Probe Taqman	56-FAM/CCATCGTAG/ZEN/GGTCCGAGGTATTC/3IABkFQ/
5S-RT/R	GATTGCAGCACCTGAGTTTCGCG
5S-F	GTTTCCCGTCCGATCAACTGTAGTTAAGC